Chemical Papers
https://doi.org/10.1007/s11696-022-02239-4

ORIGINAL PAPER

Biosynthesis of hydrophilic zinc oxide nanoparticles using *Plumeria obtusa* and *Tabernaemontana divaricata* flower extract for antidiabetic treatment

Nutan Rani[1] · Nidhi Goswami[2] · Sapna Yadav[1] · Dipak Maity[3] · Sachin Patil[4] · Kalawati Saini[1]

Received: 14 January 2022 / Accepted: 16 April 2022
© Institute of Chemistry, Slovak Academy of Sciences 2022

Abstract
A large number of people are suffering globally from diabetes due to metabolic disorders characterized by abnormally high blood sugar (glucose), which inflicts severe health issues as well as huge economic burdens. In this study, we have reported an efficient and eco-friendly biosynthesis of hydrophilic zinc oxide nanoparticles (ZnO NPs, labeled as PC1 and C1) for antidiabetic treatment using an aqueous extract of *Plumeria obtusa* and *Tabernaemontana divaricata* flowers, respectively. Phase purity, structure, morphology, and dispersibility of the as-synthesized PC1/C1 have been characterized by various analytical techniques such as UV–visible spectroscopy (UV–vis), Powder X-ray diffraction (PXRD), Fourier transform infrared spectroscopy (FTIR), thermogravimetric analysis (TGA), scanning electron microscopy (SEM), and dynamic light scattering (DLS). The UV–vis spectrum of the PC1/C1 showed maximum absorbance at ~ 370 nm and the PXRD pattern confirmed their hexagonal wurtzite crystalline structure. Besides, SEM displayed sheet and honeycomb-like shape of the PC1 and C1 while FTIR and TGA revealed the attached surface coatings of the PC1/C1. DLS results showed narrow size distribution of the PC1 and C1 in the range of 150–156 and 315–400 nm, respectively. Moreover, the zeta potential values of the as-prepared PC1 and C1 are determined as -47 and -57 mV indicating their good colloidal stability in an aqueous suspension. In vitro study has been performed to show the α-amylase inhibition activity. Furthermore, the PC1/C1 are investigated for their antidiabetic efficacy in streptozotocin (STZ)-induced diabetes in the C57BL/6 male mice. Both the PC1/C1 displayed a significant antidiabetic potential; however, the blood glucose level has been significantly reduced ($p < 0.05$) in the STZ-induced diabetic mice treated with PC1 as compared to the C1. Overall, PC1 and C1 are found to be very promising antidiabetic candidates for the in vivo antidiabetic treatment.

✉ Dipak Maity
dipakmaity@gmail.com

✉ Kalawati Saini
kalawati.saini@mirandahouse.ac.in

[1] Department of Chemistry, Miranda House, University of Delhi, New Delhi 110007, India

[2] Division of Behavioral Neurosciences, Institute of Nuclear Medicine & Allied Sciences, Delhi 110054, India

[3] Department of Chemical Engineering, University of Petroleum and Energy Studies, Dehradun 248001, India

[4] Department of Chemistry, Shiv Nadar University, Greater Noida 201314, India

Published online: 05 May 2022

Graphical abstract

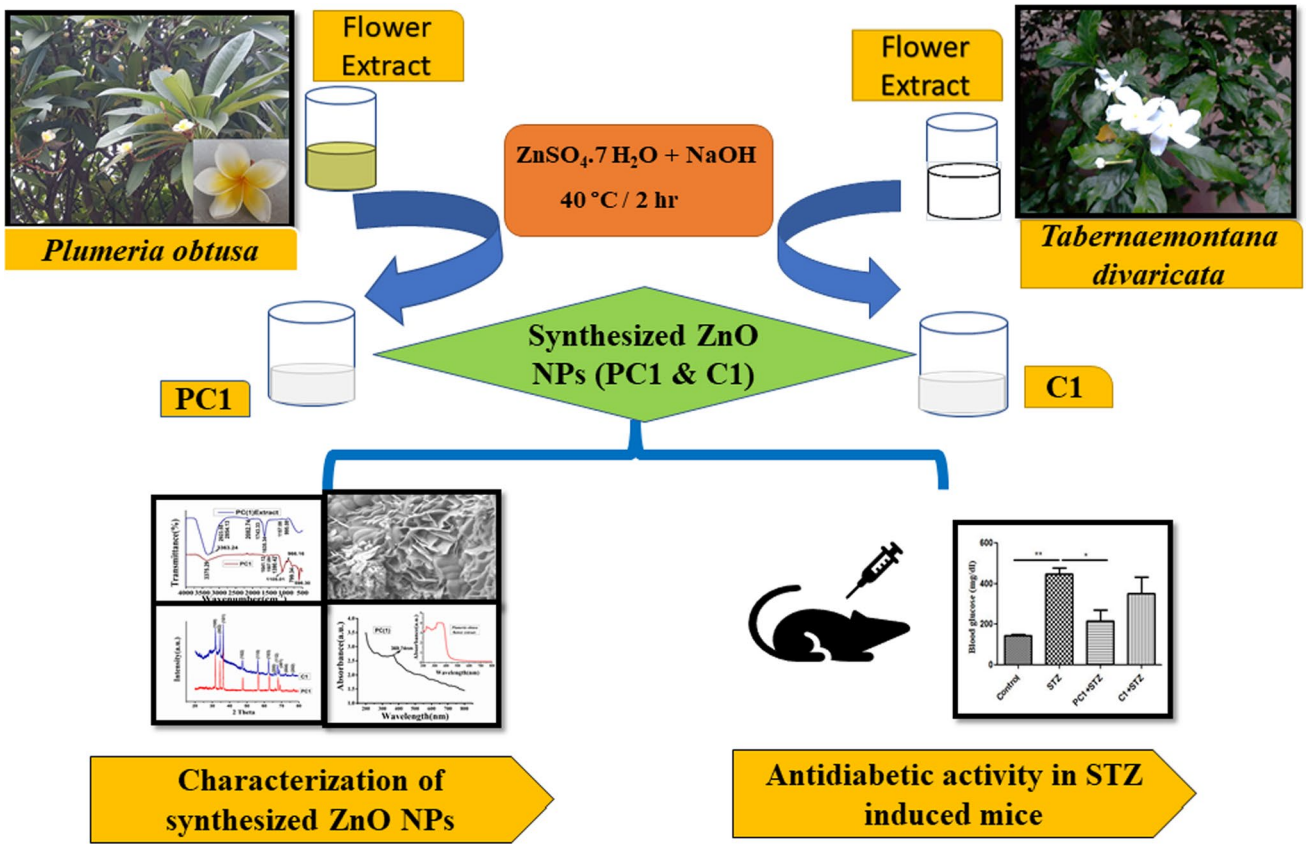

Keywords Sheet and honeycomb-shaped Zinc oxide nanoparticles · Flower extract-mediated biosynthesis · *Plumeria obtusa* · *Tabernaemontana divaricata* · Antidiabetic treatment · Streptozotocin

Introduction

Diabetes mellitus is one of the severe chronic diseases, which needs urgent attention as the number of growing incidence and prevalence of this ailment such as coronary artery disease, heart failure, and stroke have been gradually increasing over the past few decades (Maritim et al. 2003). It is a state of metabolic disorders of carbohydrate metabolism associated with high morbidity and mortality. This syndrome usually occurs due to long-term micro/macrovascular complications (such as diabetic nephropathy, diabetic foot, diabetic neuropathy, cardiovascular diseases, and diabetic retinopathy) producing deficiency of insulin hormone that regulates blood sugar/glucose levels (type 1 diabetes) or resistance of cells to insulin (type 2 diabetes) (Barik et al. 2008; Modilal and Daisy 2011). Apart from these problems, an increase in oxidative stress and a decrease in serum antioxidant enzymes such as PON-1 are thought-about common pathogenic factors of diabetogenic complications (Hussein et al. 2018). Moreover, it is considered that oxidative stress leads to severe oxidative damage to the various cell organelles like DNA (Qasim et al. 2016). Furthermore, some studies suggest the crucial role of oxidative stress in diabetes, insulin resistance, and atherosclerosis (deposition of fats, cholesterol on arteries inner walls) (Pennathur and Heinecke 2007).

Despite the availability of several traditional drugs, it is still a challenge to employ them for antidiabetic treatment because of their number of adverse effects (Hamilton. 2012). Hence, there is increased demand for natural products having antidiabetic activity due to their no or lesser side effects, low cost, and effectiveness (Carlson and Steven 1997; Atta-Ur-Rahman et al. 1989; Grover et al. 2002; Rathod et al. 2008; Akhtar et al. 2007). Moreover, according to the WHO, the medicinal plants/herbs have huge potential for diabetes treatment due to the presence of the enormous number of biologically active compounds such as terpenoids, alkaloids, proteins, vitamins, polysaccharides, phenolics, tannins, and saponins respectively (Malviya et al. 2010). Thus, extracts of various parts of the plants are exploited as both reducing and

stabilizing/capping agents for the green synthesis of metallic nanoparticles to investigate their antidiabetic activity (Saratale et al. 2018).

Currently, numerous studies have been performed using diverse biosynthesized metal/metal oxide nanoparticles to show their antidiabetic activity via the α-amylase inhibition effect. For example, the researchers have synthesized iron oxide (Fe_3O_4) nanoparticles using fruit extracts of *Annona muricata* to show their potential antidiabetic effect (Athithan et al. 2020). Similarly, nickel oxide nanoparticles using *Areca catechu* leaf extract have synthesized and found to exhibit significant antidiabetic activity (Shwetha et al. 2021). Besides, copper oxide nanoparticles (CuO NPs) are biosynthesized using the leaf extracts of *Plectranthus amboinicus,* and 94% α-amylase inhibition has been displayed at 500 µg/mL of CuO NPs (Velsankar et al. 2020). In addition, the IC_{50} value has also been reported at 317.19 µg/mL of CuO NPs. Moreover, silver oxide nanoparticles (Ag_2O NPs) are prepared using flower extract of *Zephyranthes Rosea* to exhibit 75.7% antidiabetic activity at 500 µg/mL of Ag_2O NPs using the α-amylase activity method (Maheshwaran et al. 2020). Likewise, silver nanoparticles (Ag NPs) are biosynthesized using the aqueous leaf extract of *Lonicera japonica* to demonstrate their antidiabetic activity against the carbohydrate digestive enzymes (Balan et al. 2016). In this study, IC_{50} values have been revealed at 54.56 and 37.86 µg/mL of Ag NPs due to the reticence of α-amylase and α-glucosidase, respectively.

Further, zinc is an essential metal in many metabolic processes and plays a key role in glucose utilization/metabolism besides improving insulin biosynthesis, storage, signaling, and secretion (Jansen et al. 2009). Several plant extract-mediated biosynthesis of zinc oxide (ZnO NPs) have been reported to demonstrate their enormous potential in antidiabetic applications (Nilavukkarasi et al. 2020; Jayarambabu et al. 2021; Muhammad et al. 2019; Kitture et al. 2015; Bayrami et al. 2018, 2020; Bala et al. 2015; Sati et al. 2020). For instance, Bayrami et al. studied the antidiabetic effect of biosynthesized ZnO NPs using the *Vaccinium arctostaphylos* L. leaf extract and displayed better efficacy on alloxan diabetic rats as compared to chemically synthesized ZnO NPs (Bayrami et al. 2019). There are several studies reported in the literature which highlighted the importance of zinc in maintaining the glucose homeostasis in mammals. Most of the zinc is present in the pancreatic β cells and concentrated in the dense core of insulin secreting granules (ISG). Zinc acted on insulin signalling pathway and increases hepatic glycogenesis (formation of glycogen). In this way, it inhibits the absorption of glucose by intestine and glucose uptake increases in adipose tissues and skeletal muscles (Jansen et al. 2009). Also, zinc inhibits the glucagon secretion by paracrine effect on α cells (Egefjord et al. 2010). Thereby, zinc minimizing gluconeogenesis (formation of glucose) and glycogenolysis (breaking of glycogen into glucose) processes, ultimately maintain the structural unity of insulin (Sun et al. 2009).

Uyoyo et al. also studied the effect of zinc in alloxan-induced diabetes in rats and postulated that zinc exhibited insulin like functions (Uyoyo et al. 2010). The authors also concluded that intake of zinc promotes glucose uptake and maintain hepatic functions in diabetes condition. Furthermore, *Plumeria obtusa* (known as Champa or Chafa) flowers contain various phenolic compounds that can exhibit anti-inflammatory, antipyretic, anthelmintic, antioxidant, antitumor, antiulcer, and analgesic properties (Kaisoon et al. 2011; Saleem et al. 2011; Shinde et al. 2014). Hence, *Plumeria obtusa* flowers are commonly used for the treatment of diabetes mellitus (Semenya et al. 2012; Lim 2012). Additionally, *Tabernaemontana divaricata* (known as chameli) flowers have been revealed as an anti-cancer agent (Sivaraj et al. 2014). However, the antidiabetic effects of the *Plumeria obtusa* and *Tabernaemontana divaricata* combined with ZnO NPs are not explored yet. Hence, in this work, ZnO NPs have been biosynthesized using the flower extracts of *Plumeria obtusa* (PC1) and *Tabernaemontana divaricata* (C1) to investigate their antidiabetic efficacy in streptozotocin (STZ)-induced diabetic mice.

Experimental

Materials

Zinc sulfate heptahydrate ($ZnSO_4.7H_2O$), α-amylase and sodium hydroxide (NaOH) are procured from Central Drug House (P) Ltd-CDH, India. DNSA (dinitrosalicylic acid) is procured from Loba Chemie Pvt. Ltd. Streptozotocin is obtained from Sigma Chemical Co. Ltd. UK. All the chemicals and reagents in the current study are of analytical reagent (A.R) grade and utilized with no additional purification.

Collection of plant flowers

Fresh and blossomed flowers of *Plumeria obtusa* (white Firangipani) and *Tabernaemontana divaricata* (Chameli) are collected from the garden of Miranda House, University of Delhi.

Preparation of 25% of aqueous flower extract of *Plumeria obtusa* and *Tabernaemontana divaricata*

Firstly, the *Plumeria obtusa* (white Frangipani) flowers are washed using double distilled water. These washed flowers are dried at room temperature for 30 min. 5 g of dried flowers are weighed and taken in a beaker already having 20 mL of double-distilled water. Then, the beaker is kept

on a hot plate magnetic stirrer at 40º C for 30 min. The freshly prepared *Plumeria obtusa* flower extract is filtered using Whatman filter paper number 1. A similar procedure is followed to prepare the aqueous extract of *Tabernaemontana divaricata* (Chameli) flower.

Biosynthesis of ZnO NPs

ZnO NPs are synthesized via green synthesis approach using the aqueous flower extracts of (1) *Plumeria obtusa* (ii) *Tabernaemontana divaricata*. An aqueous solution of 0.2 M pure zinc sulfate heptahydrate ($ZnSO_4.7H_2O$) is taken in a 50 ml beaker. Then, 50 mL of aqueous sodium hydroxide (NaOH) (2 M) and 1 mL freshly prepared flower extract of *Plumeria obtusa* are simultaneously added to this beaker containing zinc precursor solution with magnetic stirring (400 rpm) at 40 °C for 2 h. The resultant ZnO NPs (labelled as **PC1**) are centrifuged followed by washing with dilute alcohol and then dried at 80 °C in a hot air oven for 4 h. Similarly, the above procedure is followed for the synthesis of ZnO NPs (labelled as **C1**) with 1 ml freshly prepared flower extract of *Tabernaemontana divaricata.*

Characterization of ZnO NPs

The UV–Visible absorption spectrum of the as-prepared ZnO NPs (PC1/C1) is recorded using a UV–visible spectrophotometer (Spectromax M2e). The morphology of PC1/C1 is investigated using a field emission scanning electron microscope (FESEM) (JEOL Japan Model: JSM 6610LV) at an accelerating voltage of 30 kV. The elemental composition is measured through inbuilt energy-dispersive X-ray spectroscopy (EDS). The crystal structure and phase purity of PC1/C1 are determined by a powder X-ray diffractometer (PXRD, D8 Discover, Bruker) equipped with Cu Kα radiation ($\lambda = 0.15406$ nm) as X-ray source, with 2θ value in a range of 20°–80°. Surface coatings/functional groups attached to the ZnO NPs are identified using the FTIR spectra 55-Spectrometer (Bruker, USA) instrument. Moreover, the amount of surface coatings in PC1/C1 is determined by thermogravimetric analysis (TGA, Mettler Toledo) in the temperature range of 25–1000 °C at a rate of 20 °C/min under nitrogen atmosphere. Moreover, the hydrodynamic sizes and zeta potential values of PC1/C1 dispersed in an aqueous medium are recorded using the dynamic light scattering (DLS, Horiba Nano ZS) technique.

In vivo antidiabetic activity

In this current study, the antidiabetic activity of the biosynthesized ZnO NPs (PC1 and C1) has been studied.

Experimental animals

C57BL/6 male mice weighing ~ 25 g, 8–12 weeks old, are taken from an inbred colony from an experimental animal facility maintained under a 12-h light/12-h dark cycle, temperature 22 ± 1 °C, with ad libitum food and water. Animals are acclimatized to the laboratory conditions for 1 week prior to the study. The research is conducted with the approval of the institute's animal ethics committee. The abovementioned particular age is chosen to decrease the streptozotocin sensitivity. The effect of streptozotocin dose has been studied on the different age groups of rats (Masiello et al. 1979). Herein, higher sensitivity has been investigated in very young rats.

Experimental design and diabetes induction

The diabetic model is prepared using the procedure with slight modification as described previously by the researchers. (Alkaladi et al. 2014). Briefly, food pellets are removed from the cage 4 h prior to the experiment (Day 1). Streptozotocin (STZ, an antibiotic isolated from streptomyces achromogenes in 1960) is dissolved immediately before the experiment in sodium citrate buffer (50 mM) to a final concentration of 4 mg/ml. STZ (40 mg/kg) is injected intraperitoneally using a 25-gauge, 1 mL syringe. An equal amount of citrate buffer (pH = 4.5) is injected into the control group. Mice are returned to home cages and provided with 10% sucrose water. The process is repeated for the next 4 consecutive days. On day 6, 10% sucrose is replaced with normal water. On day 14, blood glucose levels are checked for hyperglycemic conditions in STZ-treated mice. The blood sample is taken from the tail vein of the mice. After that the glucose in the blood sample is analyzed using a One Torch Basic blood glucose monitoring system to ensure hyperglycemia in STZ treated mice group.

Out of 26, 18 animals are found to have blood glucose levels higher than 150 mg/dL. Hyperglycemic animals are carried further for testing the antidiabetic effect of the drug.

Groups are divided as follows: Group I (Control mice), Group II (STZ treated), Group III (STZ + PC1, 10 mg/kg), and Group IV (STZ + C1, 10 mg/kg), $N = 6$ each group. Mice have received drugs orally once daily for seven days. At the end of the experiment, blood glucose levels are measured in all groups.

Statistical analysis

Data are analyzed using one-way analysis of variance (ANOVA using Graphpad prism 8 software), followed by Dunnett's post hoc analysis and represented as mean ± SEM. Difference between groups is considered significant at $p < 0.05$.

In vitro α-amylase inhibitory assay

The α-amylase inhibitory activity of the green synthesized ZnO nanoparticles (PC1 and C1) was carried out using the standard protocol with slight modifications. (Kazeem et al. 2013).

Briefly, 50 µL of the α-amylase solution was mixed with different concentrations (100–500 µg/mL) of green synthesized ZnO nanoparticles (PC1 and C1), acarbose (a drug used as such) as standard and a control (without standard/test samples) in a 96 well microtiter plate. Then after 10 min, 50 µL of the starch solution was added to each well. The well plate was incubated at 37 °C for 30 min. Subsequently, 100 µL of dinitrosalicylic acid (DNSA) was added to each well. After that, the well plate was incubated at 90 °C for 10 min and then cooled. Finally, the absorbance was measured at 540 nm using a Spectromax M2e spectrophotometer. Using the following equation, % inhibition of α-amylase activity was calculated.

$$\% \text{ Inhibition} = \left(\left[\text{Abs(control)} - \text{Abs (sample)}\right]/[\text{Abs (control)}]\right) \times 100$$

Results and discussions

UV–Visible spectroscopic analysis

UV–visible (UV–vis) analysis has been conducted to confirm the formation of green synthesized ZnO nanoparticles using the flower extract of *Plumeria obtusa* (PC1) and *Tabernaemontana divaricata* (C1). Figures 1a and 2a show the UV–vis spectra of the biosynthesized PC1 and C1 while recorded in the range of 200–800 nm at room temperature.

The sharp peak obtained, respectively, at 369.74 and 370 nm in Fig. 1a and 2a confirm the formation of ZnO nanoparticles for both the case of PC1 and C1 synthesis. The obtained value of absorption maximum wavelength matches well with the value reported by many authors. (Jayappa et al. 2020; El-Belely et al. 2021). A similar value has been also obtained by Saeed et al. where ZnO NPs are synthesized using the *Achyranthes aspera* leaf extract (Saeed et al. 2021). Moreover, the UV–vis spectra have been recorded for the only flower extract of *Plumeria obtusa* and *Tabernaemontana divaricata* as shown in the insets of Figs. 1a and 2a, respectively.

Figures 1b and 2b depict the corresponding tauc plot determined from the UV–visible spectroscopic data. By using the following Eq. (1), the value of the energy bandgap

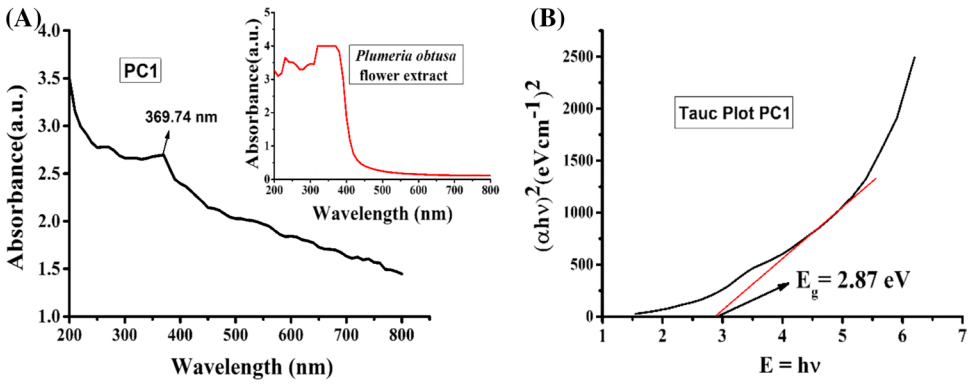

Fig. 1 (**A**) UV–Visible absorption spectra of biosynthesized ZnO NPs using *Plumeria obtusa* (PC1) and extract of *Plumeria obtusa* flowers (inset) and (**B**) Tauc plot $(\alpha h\nu)^2$ vs $h\nu$ (eV) of PC1

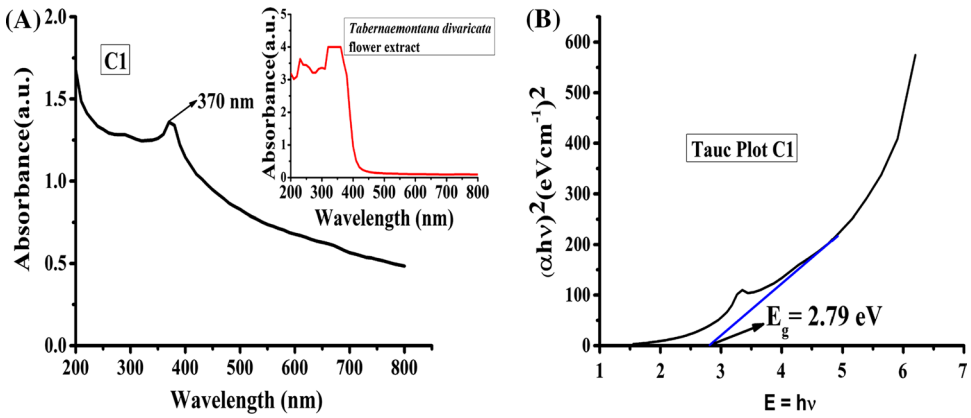

Fig. 2 (**A**) UV–Visible absorption spectra of biosynthesized ZnO NPs using *Tabernaemontana divaricata* (C1) and extract of *Tabernaemontana divaricata* flowers and (**B**) Tauc plot $(\alpha h\nu)^2$ vs $h\nu$ (eV) of C1

(E_g) is found to be 2.87 and 2.79 eV for the PC1 and C1, respectively, where A is a constant, α is the absorption coefficient, E_g is the band gap energy and hν is the photon energy in the Eq. 1.

$$(\alpha h\nu)^2 = A\left(h\nu - E_g\right)^{1/2} \quad (1)$$

FTIR analysis

FTIR spectrum has been recorded in the range of 4000–400 cm^{-1} to investigate the presence of functional groups attached to the as-synthesized ZnO NPs (PC1 and C1) and also in the only extract of the *Plumeria Obtusa* and *Tabernaemontana divaricata* flowers. Figure 3a shows the FTIR spectrum of the PC1 and the extract of the *Plumeria Obtusa* flowers. The FTIR spectrum of *Plumeria Obtusa* flower extract exhibited bands at 3363.24, 2923.55, 2854.13, 2082.74, 1743.33, 1635.34, 1157.08, and 995.08 cm^{-1} due to the presence of a large number of biomolecules like polyphenols and flavonoids. Similarly, the spectrum of the PC1 showed the bands at 3375.29, 1641.12,1507.09, 1390.42, 1105.01, 966.16, and 799.34 cm^{-1} corresponding to -OH stretching vibration of phenol and water molecules, –C=C– stretching vibrations of aromatic compounds, –C=C vibrations of alkyl ethers, –COO stretching vibration and -C-O stretched aromatic and aliphatic amines, respectively (Govindan et al. 2020).

Figure 3b depicts the FTIR spectrum of the as-synthesized ZnO NPs (C1) and also in the extract of the *Tabernaemontana divaricata* flowers. The FTIR spectrum of *Tabernaemontana divaricata* flower extract shows bands at 3316.96 and 1637.26 cm^{-1} due to the presence of –OH stretching vibration of phenolic groups and stretching vibration of –C=C– bonds of aromatic compounds, respectively. Similarly, the spectrum of the C1 showed the bands at 3336.24, 1631.48, 1097.29, 968.09, and 796.45 cm^{-1} corresponding to -OH stretching vibration of phenolic groups, -C=C- stretching vibration of alkyl ethers, -C-O stretch of ether, -carboxylic acid group and -C-N stretching vibrations of amines, respectively (Happy et al. 2019; Sendhil et al. 2021). Furthermore, the bands observed in the range of 500–700 cm^{-1} are associated with the presence of Zn–O bonds.

Thus, FTIR spectra (Fig. 3a and b) confirmed that the surface of the as-synthesized ZnO NPs (PC1/C1) are attached with coatings of the biomolecules from the extracts of *Plumeria Obtusa* and *Tabernaemontana divaricata* flowers. Additionally, it indicates that the flower extract coatings (of PC1 and C1) contain both carboxylate and hydroxyl functionality, which not only capped the ZnO nanoparticles but is also available for further bio-conjugation at their surface periphery.

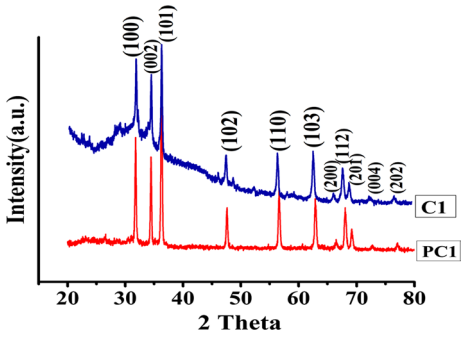

Fig. 4 Powder X-ray diffraction pattern as-prepared ZnO NPs using the flower extracts of *Plumeria obtusa* (PC1) and *Tabernaemontana divaricata* (C1)

Powder X-Ray Diffraction (PXRD) analysis

Figure 4 depicts the PXRD pattern of the as-synthesized ZnO NPs (PC1 and C1). The major peaks have been observed at the 2θ values of 31.8°, 34.4°, 36.2°, 47.6°, 56.6°, 62.9°, 66.4°, 68.0°, 69.1° for PC1 and at 2θ values of 31.7°, 34.4°, 36.2°, 47.5°, 56.5°, 62.8°, 66.3°, 67.9°, 69.0° for C1, respectively, corresponding to the *hkl* planes (100), (002), (101), (102), (110), (103), (200), (112), (201), (004) and (202). Thus, the 2θ values and corresponding (*hkl*) planes

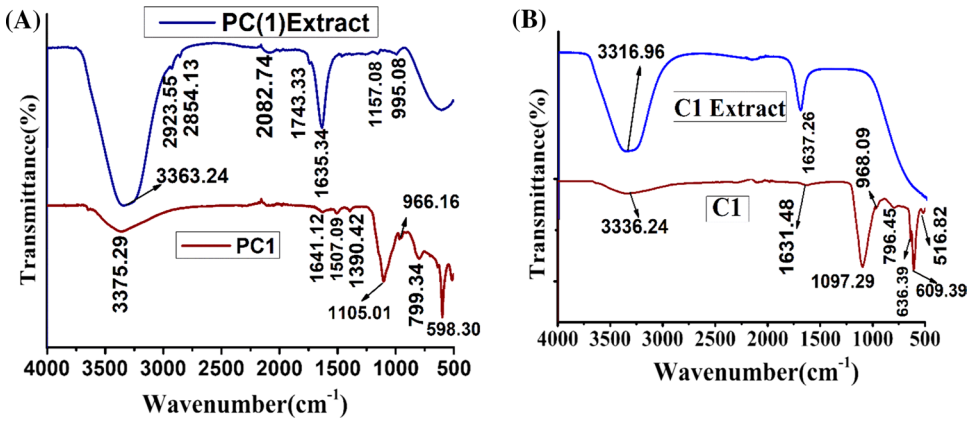

Fig. 3 (**A**) FTIR spectrum of biosynthesized ZnO NPs using *Plumeria obtusa* (PC1) and extract of *Plumeria obtusa* flowers and (**B**) FTIR spectrum of biosynthesized ZnO NPs using *Tabernaemontana divaricata* (C1) and only extract of *Tabernaemontana divaricata* flowers

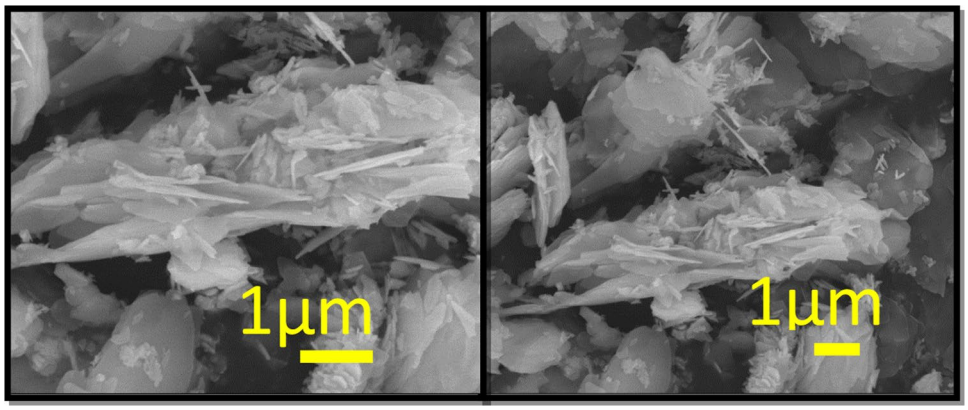

Fig. 5 SEM Spectra for biosynthesized ZnO NPs using *Plumeria obtusa* (PC1)

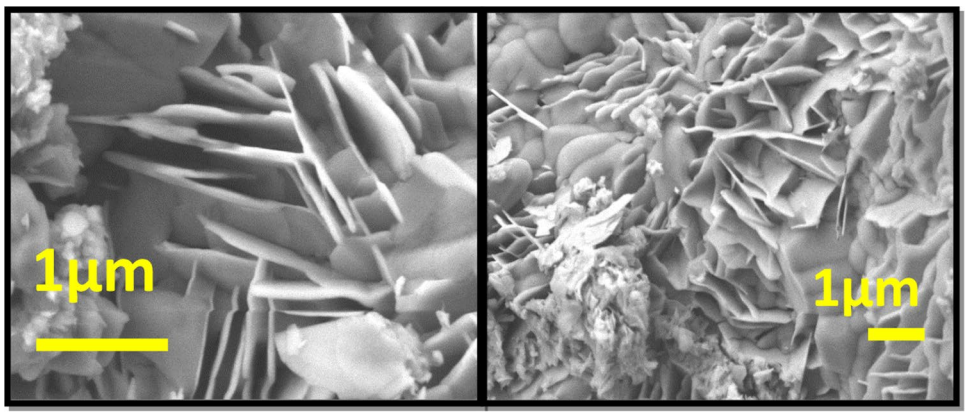

Fig. 6 SEM Spectra for biosynthesized ZnO NPs using *Tabernaemontana divaricata* (C1)

in the PXRD pattern confirm the hexagonal wurtzite polycrystalline structure of the PC1/C1. Moreover, the observed PXRD spectra match well with the diffraction pattern reported in the literature. (Abdelkhalek and Al-Askar 2020). The more intense and sharp peaks show that as-synthesized ZnO NPs are highly crystalline in nature. Furthermore, the phase purity of the PC1 and C1 is confirmed due to the absence of any peak related to the impurities.

SEM and EDS analysis

Figures 5 and 6 show the SEM images of the as-synthesized ZnO NPs synthesized using flower extract of *Plumeria obtusa* and *Tabernaemontana divaricata*, respectively. It can be seen that the SEM micrographs have revealed the stacked thin nanosheets and honeycomb-like structures of the PC1 and C1, respectively. The similar morphology of the ZnO NPs has also reported by various authors. (Kakiuchi et al. 2006; Ardakani and Rafieipour 2018). Tables 1 and 2 show the EDS analysis of the as-prepared ZnO nanoparticles.

Table 1 Energy Dispersive Spectroscopy (EDS) analysis of as-synthesized ZnO NPs (PC1)

Element	Weight %	Atomic %	Net Int	Error %
O K	31.74	65.51	314.96	4.03
Zn K	68.26	34.49	52.41	7.68

Table 2 Energy Dispersive Spectroscopy (EDS) analysis of as-synthesized ZnO NPs (C1)

Element	Weight %	Atomic %	Net Int	Error %
OK	36.10	69.78	73.37	5.03
Zn K	63.90	30.22	9.79	15.90

TGA and zeta potential analysis

Figure 7a and b show the TGA and zeta potential plots of the ZnO NPs synthesized using the flower extracts of *Plumeria obtusa* (PC1) and *Tabernaemontana divaricata* (C1), respectively. TGA plots showed three stages of weight losses of the samples with the temperature as shown in Fig. 7a. The initial weight loss in the temperature range between 25–250 °C is attributed to the

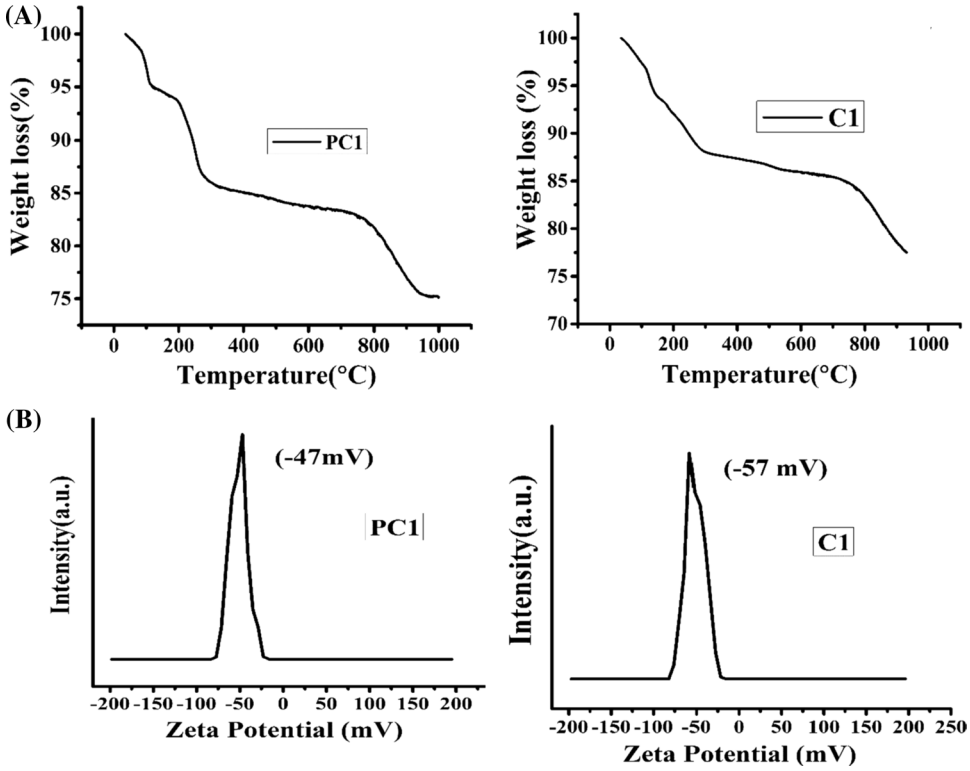

Fig. 7 (**A**) TGA and (**B**) zeta potential plots of biosynthesized ZnO NPs using the flower extracts of *Plumeria obtusa* (PC1) and *Tabernaemontana divaricata* (C1)

evaporation of physically adsorbed (loosely bound) water molecules. The second weight loss in the temperature range between 250 and 780 °C is associated with the chemically adsorbed (strongly bound) organic surface coating attached to the surface of ZnO NPs. Moreover, the weight loss occurred very slowly suggesting the polymeric nature of the plant extract and significant interactions between the coating and the NPs. The final weight loss in the range between ~ 790 and 1000 °C is due to the complete decomposition of the organic coating from the surface of the NPs. The total weight loss is observed as 25% in the case of PC1 and 28% in the case of C1. It is reported that the bare ZnO NPs decompose only 4–5% in the temperature range 25–1000 °C (Chunduri et al. 2017). This indicates a nearly 20 and 23 wt% organic coatings are attached to the PC1 and C1, respectively.

The zeta potential signs and values of the ZnO NPs represent the type of surface charge and colloidal stability of the NPs, respectively. The zeta potential values are determined as -47 mV for PC1 and -57 mV for C1, respectively, as shown in Fig. 7b. These results closely match with the zeta potential value of -53.5 mV for the green synthesized ZnO NPs using *Proteus mirabilis* strain 10B. (Eltarahony et al. 2018). Thus, zeta potential values are found to be greater than -30 mV indicating high colloidal stability of the ZnO NPs in their aqueous suspension.

Particle size distribution

The DLS technique has been used to determine the particle size distribution of the as-synthesized PC1 and C1 dispersed in an aqueous media. Figure 8a shows the hydrodynamic sizes in the range of 150–156 nm for the PC1, whereas Fig. 8b shows the hydrodynamic sizes in the range of 315–400 nm for the C1. Thus, the PC1 have revealed smaller size with relatively more narrow size distribution as compared to the C1 due to their different thickness of the hydrodynamical shell which depends on the roughness, shape, and structure of the NPs (Kätzel et al. 2008).

Antidiabetic activities

(a) *α-amylase inhibition activity*

α-amylase and α-glucosidase are carbohydrate hydrolyzing enzymes that are responsible for postprandial hyperglycemia. Type 2 diabetes is due to the imbalance between blood sugar absorption and insulin secretion. Postprandial hyperglycemia plays a key role in the development of type 2 diabetes. The ability of a drug to slow down the production or absorption of glucose by inhibiting the abovementioned enzymes can be of great use for the management of diabetes

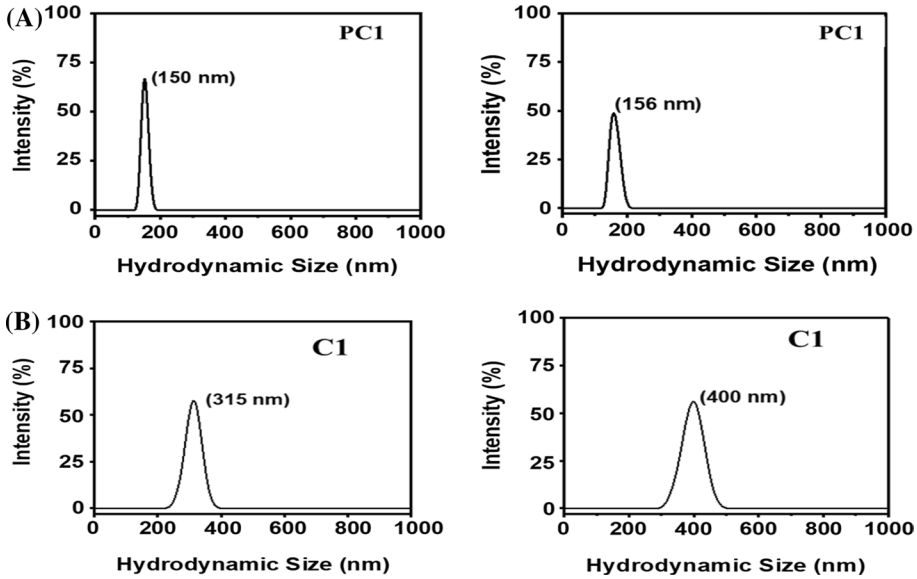

Fig. 8 Hydrodynamic size of the biosynthesized (**A**) PC1 and (**B**) C1 nanoparticles dispersed in an aqueous suspension

mellitus or its prevention. Figure 9 shows the % inhibition of α-amylase with the varied concentration (100–500 µg/mL) of zinc oxide nanoparticles (PC1 and C1) and also with the drug acarbose which is used as standard. It is clear from the Fig. 9 that the inhibition effect of PC1 NPs has been found more as compared to C1 NPs.

(b) *Fasting Blood Sugar*

Figure 10 shows the graph where the antidiabetic activity of *Plumeria obtusa* flower extract (1 mL)-mediated ZnO NPs (PC1) and *Tabernaemontana divaricata* flower extract (1 mL)-mediated ZnO NPs (C1) with changes in blood glucose level post-treatment is displayed. The obtained results indicate that the blood glucose level is increased in the STZ provoked diabetic mice ($p < 0.001$) in comparison to the control group. Moreover, the blood glucose level is significantly reduced ($p < 0.05$) for the STZ-induced diabetic mice treated with PC1. However, relatively less difference in the blood glucose level is obtained for the STZ-induced diabetic mice treated with C1.

The STZ increased the blood glucose level to 500 mg/dL, compared with 144 mg/dL in normal control mice. Moreover, intraperitoneal injection of ZnO NPs (PC1) in STZ-induced mice decreases the blood glucose level to 213 mg/dL compared to ZnO NPs (C1) which decreases the blood glucose level to 344 mg/dL only.

Our results are matched with reported antidiabetic activity in the literature (Siddiqui et al. 2020; Virgen-Ortiz et al. 2020). For instance, Siddiqui et al. have found that

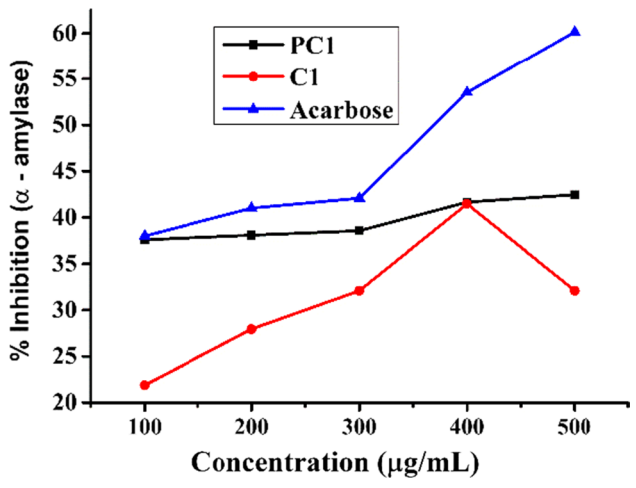

Fig. 9 Graph shows the % inhibition of α-amylase with the varied concentration (100–500 µg/mL) of zinc oxide nanoparticles (PC1 and C1) and also with the drug acarbose which is used as the standard

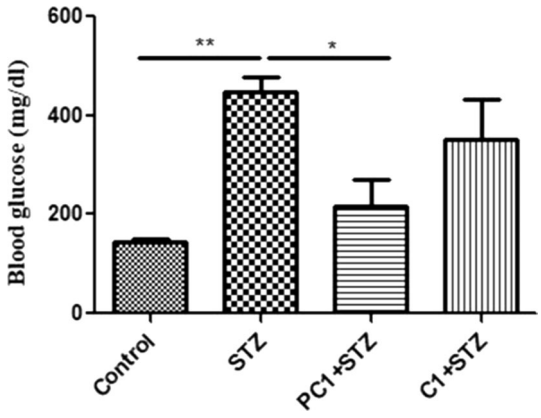

Fig. 10 Graph shows the antidiabetic potential of *Plumeria obtusa* flower extract (1 ml)-mediated ZnO NPs (PC1) and *Tabernaemontana divaricata* flower extract (1 mL)-mediated ZnO NPs (C1) with changes in blood glucose level post-treatment. Control group is treated with citrate buffer (pH = 4.5) and STZ group is treated with dose of streptozotocin means no drug is given to cure

utilization of ZnO NPs in the STZ-induced diabetic mice resulted in a significant decrease in the value of fasted blood glucose level. They have also conducted the hypoglycemic activity test and OGTT (oral glucose tolerance test). In the hypoglycemic test, ZnO NPs have reduced the blood glucose levels by 25.13 and 29.15% at two doses of 8 and 14 mg/kg body weight of mice. Virgen- Ortiz et al. studies have also suggested that the ZnO NPs induce an acute hyperglycemic effect in normal and diabetic rats. Also, the hyperglycemic effect depends on the dose amount and the route of administration. Li et al. have used Pt NPs for the antidiabetic application in streptozotocin-induced diabetic rats (Li et al. 2017). These Pt NPs have been synthesized using the leaves extract of *Whitania somnifers*. These NPs decreased the level of glucose in plasma to 117.34 ± 4.18 mg/dL.

Conclusion

Hydrophilic sheet and honeycomb-shaped ZnO NPs have been successfully biosynthesized using flower extracts of *Plumeria obtusa* (PC1) and *Tabernaemontana divaricata* (C1). The as-synthesized PC1/C1 have shown relatively narrow size distribution (150–156 and 315–400 nm) while exhibiting high colloidal stability in an aqueous medium. In vitro study has been done for the % inhibition activity of α-amylase with change in the concentration of zinc oxide nanoparticles (PC1 and C1). This in vitro study reveals that the inhibition effect of PC1 NPs has been obtained more as compared to C1 NPs. In vivo antidiabetic studies of the PC1/C1-coated ZnO NPs have been performed using streptozotocin-induced diabetic mice models. A significant increase in blood glucose level (more than 250 mg/dL) is observed after intraperitoneal injection of streptozotocin. Our results indicated that PC1 and C1 significantly reduced the blood glucose levels in STZ-induced diabetic mice. Moreover, the reduction in blood glucose level is found to be more prominent for the mice treated with PC1 as compared to C1. To summarize, biosynthesized metal oxide nanoparticles-based antidiabetic drugs can be a better alternative in order to minimize the adverse side effects caused by the use of traditional antidiabetic drugs.

Acknowledgements The authors are grateful to Principal, Miranda House, University of Delhi, for providing the lab facility to carry out this research work. Dipak Maity would like to thank the University of Petroleum and Energy Studies (UPES) for providing all the supports. The authors would like to thank Kailash Manda, Scientist-F, Division of Behavioral Neurosciences, Institute of Nuclear Medicine & Allied Sciences, Delhi-110054, India, for validating the antidiabetic activity results. The authors would also like to thank Bimlesh Lochab, Shiv Nadar University, for TGA measurements. The authors wish to thank USIC, University Scientific Instrumentation Centre, University of Delhi, India, for providing FTIR, PXRD facilities.

References

Abdelkhalek A, Al-Askar AA (2020) Green synthesized ZnO nanoparticles mediated by *Mentha Spicata* extract induce plant systemic resistance against tobacco mosaic virus. Appl Sci 10(15):5054. https://doi.org/10.3390/app10155054

Akhtar MA, Rashid M et al (2007) Comparison of long-term antihyperglycemic and hypolipidemic effects between *Coccinia cordifolia* (Linn.) and *Catharanthus roseus* (Linn.) in alloxan-induced diabetic rats. Res J Med Med Sci 2(1):29–34

Alkaladi A, Abdelazim AM et al (2014) Antidiabetic activity of zinc oxide and silver nanoparticles on Streptozotocin-induced diabetic rats. Int J Mol Sci 15(2):2015–2023. https://doi.org/10.3390/ijms15022015

Ardakani AG, Rafieipour P (2018) Using ZnO nanosheets grown by electrodeposition in random lasers as scattering centers: the effects of sheet size and presence of mode competition. J Opt Soc Am B 35(7):1708–1716. https://doi.org/10.1364/JOSAB.35.001708

Athithan AS, Jeyasundari J et al (2020) *Annona muricata* fruit mediated biosynthesis, physicochemical characterization of magnetite (Fe3O4) nanoparticles and assessment of its in vitro antidiabetic activity. Rasayan J Chem 13(3):1759–1766. https://doi.org/10.31788/RJC.2020.1335789

Atta-Ur-Rahman ZK et al (1989) Medicinal plants with hypoglycemic activity. J Ethnopharmacol 26(1):1–5. https://doi.org/10.1016/0378-8741(89)90112-8

Bala N, Saha S et al (2015) Green synthesis of zinc oxide nanoparticles using Hibiscus subdariffa leaf extract: effect of temperature on synthesis, anti-bacterial activity and anti-diabetic activity. RSC Adv 5(7):4993–5003. https://doi.org/10.1039/C4RA12784F

Balan K, Qing W et al (2016) Antidiabetic activity of silver nanoparticles from green synthesis using *Lonicera japonica* leaf extract. RSC Adv 6(46):40162–40168. https://doi.org/10.1039/C5RA24391B

Barik R, Jain S et al (2008) Antidiabetic activity of aqueous root extract of *Ichnocarpus frutescens* in streptozotocin-nicotinamide induced type-II diabetes in rats. Indian J Pharmacol 40(1):19–22. https://doi.org/10.4103/0253-7613.40484

Bayrami A, Parvinroo S et al (2018) Bio-extract-mediated ZnO nanoparticles: microwave-assisted synthesis, characterization and antidiabetic activity evaluation. Artif Cells Nanomed Biotechnol 46(4):730–739. https://doi.org/10.1080/21691401.2017.1337025

Bayrami A, Alioghli S et al (2019) A facile ultrasonic-aided biosynthesis of ZnO nanoparticles using *Vaccinium arctostaphylos L.* leaf extract and its antidiabetic, antibacterial, and oxidative activity evaluation. Ultrason Sonochem 55:57–66. https://doi.org/10.1016/j.ultsonch.2019.03.010

Bayrami A, Haghgooie S et al (2020) Synergistic antidiabetic activity of ZnO nanoparticles encompassed by *Urtica dioica* extract. Adv Powder Technol 31:2110–2118. https://doi.org/10.1016/j.apt.2020.03.004

Carlson TJ, Steven RK (1997) From plant to patient: an ethnomedical approach to the identification of new drugs for the treatment of NIDDM. Diabetologia 40:614–617. https://doi.org/10.1007/s001250050724

Chunduri LAA, Kurdekar A et al (2017) Streptavidin conjugated ZnO nanoparticles for early detection of HIV infection. Adv Mater Lett 8(4):472–480. https://doi.org/10.5185/amlett.2017.6579.

Egefjord L, Petersen AB et al (2010) Zinc, alpha cells and glucagon secretion. Curr Diabetes Rev 6(1):52–57. https://doi.org/10.2174/157339910790442655.

El-Belely EF, Farag MMS et al (2021) Green synthesis of zinc oxide nanoparticles (ZnO-NPs) Using *Arthrospira platensis* (Class: Cyanophyceae) and evaluation of their biomedical activities. Nanomaterials 11(1):95. https://doi.org/10.3390/nano11010095

Eltarahony M, Zaki S et al (2018) Biosynthesis, characterization of some combined nanoparticles, and its biocide potency against a broad spectrum of pathogens. J Nanomater 2018:5263814. https://doi.org/10.1155/2018/5263814

Govindan N, Vairaprakasam K et al (2020) Green synthesis of Zn-doped *Catharanthus Roseus* nanoparticles for enhanced anti-diabetic activity. Mater Adv 1(9):3460–3465. https://doi.org/10.1039/D0MA00698J

Grover JK, Yadav S et al (2002) Medicinal plants of India with anti-diabetic potential. J Ethnopharmacol 81(1):81–100. https://doi.org/10.1016/S0378-8741(02)00059-4

Hamilton CA (2012) Pharmacological management of type 2 diabetes mellitus in patients with CKD. J Ren Care 38:59–66. https://doi.org/10.1111/j.1755-6686.2012.00275.x

Happy A, Soumya M et al (2019) Phyto-assisted synthesis of zinc oxide nanoparticles using *Cassia alata* and its antibacterial activity against Escherichia coli. Biochem Biophys Rep 17:208–211. https://doi.org/10.1016/j.bbrep.2019.01.002

Hussein J, El-Banna M et al (2018) Biocompatible zinc oxide nanocrystals stabilized via hydroxyethyl cellulose for mitigation of diabetic complications. Int J Biol Macromol 107:748–754. https://doi.org/10.1016/j.ijbiomac.2017.09.056

Jansen J, Karges W et al (2009) Zinc and diabetes—clinical links and molecular mechanisms. J Nutr Biochem 20(6):399–417. https://doi.org/10.1016/j.jnutbio.2009.01.009

Jayappa MD, Ramaiah CK et al (2020) Green synthesis of zinc oxide nanoparticles from the leaf, stem and in vitro grown callus of *Mussaenda frondosa L.*: characterization and their applications. Appl Nanosci 10(8): 3057–3074. https://doi.org/10.1007/s13204-020-01382-2

Jayarambabu N, Rao TV et al (2021) Anti-hyperglycemic, pathogenic and anticancer activities of *Bambusa arundinacea* mediated zinc oxide nanoparticles. Mater Today Commun 26:101688. https://doi.org/10.1016/j.mtcomm.2020.101688

Kaisoon O, Siriamornpun S et al (2011) Phenolic compounds and anti-oxidant activities of edible flowers from Thailand. J Funct Food 3(2):88–99. https://doi.org/10.1016/j.jff.2011.03.002

Kakiuchi K, Hosono E et al (2006) Fabrication of mesoporous ZnO nanosheets from precursor templates grown in aqueous solutions. J Sol-Gel Sci Techn 39(1):63–72. https://doi.org/10.1007/s10971-006-6321-6

Kätzel U, Vorbau M et al (2008) Dynamic light scattering for the characterization of polydisperse fractal systems: II. Relation between structure and DLS results. Part Part Syst Charact 25(1):19–30 .https://doi.org/10.1002/ppsc.200700005

Kazeem MI, Adamson JO et al (2013) Modes of inhibition of α-amylase and α-glucosidase by aqueous extract of Morinda lucida Benth leaf. Biomed Res Int. https://doi.org/10.1155/2013/527570

Kitture R, Chordiya K et al (2015) ZnO Nanoparticles-red sandalwood conjugate: a promising anti-diabetic agent. J Nanosci Nanotechnol 15(6):4046–4051. https://doi.org/10.1166/jnn.2015.10323

Li Y, Zhang J et al (2017) Biosynthesis of polyphenol-stabilised nanoparticles and assessment of anti-diabetic activity. J Photochem Photobiol B Biol 169:96–100. https://doi.org/10.1016/j.jphotobiol.2017.02.017

Lim TK (2012) Edible medicinal and non-medicinal plants. Springer, Dordrecht

Maheshwaran G, Bharathi AN et al (2020) Green synthesis of Silver oxide nanoparticles using *Zephyranthes Rosea* flower extract and evaluation of biological activities. J Environ Chem Eng 8(5):104137. https://doi.org/10.1016/j.jece.2020.104137

Malviya N, Jain S et al (2010) Antidiabetic potential of medicinal plants. Acta Pol Pharm 67(2):113–118

Maritim AC, Sanders RA et al (2003) Diabetes, oxidative stress, and antioxidants: a review. J Biochem Mol Toxicol 17(1):24–38. https://doi.org/10.1002/jbt.10058

Masiello P, De Paoli AA et al (1979) Influence of age on the sensitivity of the rat to streptozotocin. Horm Res Paediatr 11(5):262–274. https://doi.org/10.1159/000179062

Modilal MRD, Daisy P (2011) Hypoglycemic effects of Elephantopus scaber in Alloxan-induced diabetic rats. Indian J Nov Drug Deliv 3:93–103

Muhammad W, Ullah N et al (2019) Optical, morphological and biological analysis of zinc oxide nanoparticles (ZnO NPs) using *Papaver somniferum* L. RSC Adv 9(51):29541–29548. https://doi.org/10.1039/C9RA04424H

Nilavukkarasi M, Vijayakumar S et al (2020) *Capparis zeylanica* mediated bio-synthesized ZnO nanoparticles as antimicrobial, photocatalytic and anti-cancer applications. Mater Sci Energy Technol 3:335–343. https://doi.org/10.1016/j.mset.2019.12.004

Pennathur S, Heinecke JW (2007) Mechanisms for oxidative stress in diabetic cardiovascular disease. Antioxid Redox Signal 9(7):955–969. https://doi.org/10.1089/ars.2007.1595

Qasim M, Bukhari SA et al (2016) Relationship of oxidative stress with elevated level of DNA damage and homocysteine in cardiovascular disease patients. Pak J Pharm Sci 29(6):2297–2302

Rathod N, Raghuveer I et al (2008) Antidiabetic activity of *Nyctanthes arbortristis*. Phcog Mag 4(16):40–64

Saeed S, Nawaz S et al (2021) Effective fabrication of zinc-oxide (ZnO) nanoparticles using *Achyranthes aspera* leaf extract and their potent biological activities against the bacterial poultry pathogens. Mater Res Express 8(3):035004. https://doi.org/10.1088/2053-1591/abea47

Saleem M, Akhtar N et al (2011) Isolation and characterization of secondary metabolites from *Plumeria obtusa*. J Asian Nat Prod Res 13(12): 1122–1127 .https://doi.org/10.1080/10286020.2011.618452

Saratale RG, Saratale GD et al (2018) New insights on the green synthesis of metallic nanoparticles using plant and waste biomaterials: current knowledge, their agricultural and environmental applications. Environ Sci Pollut Res 25(11):10164–10183. https://doi.org/10.1007/s11356-017-9912-6

Sati SC, Kour G et al (2020) Biosynthesis of metal nanoparticles from leaves of *Ficus palmata* and evaluation of their anti-inflammatory and anti-diabetic activities. Biochemistry 59:3019–3025. https://doi.org/10.1021/acs.biochem.0c00388

Semenya S, Potgieter M et al (2012) Ethnobotanical survey of medicinal plants used by Bapedi healers to treat diabetes mellitus in the Limpopo province. South Africa J Ethnopharmacol 141(1):440–445. https://doi.org/10.1016/j.jep.2012.03.008

Sendhil M, Sindhuja K et al (2021) Green synthesis of zinc oxide nanoparticles from *camellia sinensis*: organic dye degradation, antibacterial activity and in silico studies. Inorg Chem Commun, 108956. https://doi.org/10.1016/j.inoche.2021.108956

Shinde PR, Patil PS et al (2014) Phytopharmacological review of *Plumeria* species. Sch Acad J Pharm 3(2):217–227

Shwetha UR, Kumar CRR et al (2021) Biogenic synthesis of NiO nanoparticles using *Areca catechu* leaf extract and their antidiabetic and cytotoxic effects. Molecules 26(9):2448. https://doi.org/10.3390/molecules26092448

Siddiqui SA, Or Rashid MM et al (2020) Biological efficacy of zinc oxide nanoparticles against diabetes: a preliminary study conducted in mice. Biosci Rep 40(4):BSR20193972. https://doi.org/10.1042/BSR20193972

Sivaraj R, Rahman PKSM et al (2014) Biogenic zinc oxide nanoparticles synthesis using *Tabernaemontana divaricata* leaf extract and its anticancer activity against MCF-7 breast cancer cell Lines. In: International Conference on Advances in Agricultural, Biological & Environmental Sciences 2014. https://doi.org/10.15242/IICBE.C1014032

Sun Q, Van Dam RM et al (2009) Prospective study of zinc intake and risk of type 2 diabetes in women. Diabetes Care 32(4):629–634. https://doi.org/10.2337/dc08-1913

Uyoyo Ukperoro J, Offiah N et al (2010) Antioxidant effect of zinc, selenium and their combination on the liver and kidney of alloxan-induced diabetes in rats. Mediterr J Nutr Metab 3(1):25–30. https://doi.org/10.3233/s12349-009-0069-9

Velsankar K, Vinothini V et al (2020) Green synthesis of CuO nanoparticles via *Plectranthus amboinicus* leaves extract with its characterization on structural, morphological and biological properties. Appl Nanosci 10(10):3953–3971. https://doi.org/10.1007/s13204-020-01504-w

Virgen-Ortiz A, Apolinar-Iribe A et al (2020) Zinc oxide nanoparticles induce an adverse effect on blood glucose levels depending on the dose and route of administration in healthy and diabetic rats. Nanomaterials 10(10):2005. https://doi.org/10.3390/nano10102005

Publisher's Note Springer Nature remains neutral with regard to jurisdictional claims in published maps and institutional affiliations.